Chemical Engineering Journal 234 (2013) 266–275

Contents lists available at ScienceDirect

Chemical Engineering Journal

journal homepage: www.elsevier.com/locate/cej

Kinetic study of methyl-butenes dimerization and trimerization in liquid-phase over a macroreticular acid resin

Marta Granollers, José F. Izquierdo, Carles Fité, Fidel Cunill *

Chemical Engineering Department, Faculty of Chemistry, University of Barcelona, Spain

HIGHLIGHTS

- LHHW–ER kinetic models fitted isoamylene dimers and trimers formation reaction rates.
- In isoamylene dimerization was implied one active site or cluster of active sites.
- In isoamylene trimerization were implied three active sites or clusters.
- The adsorption terms of isoamylene, dimer and *n*-hexane were implied in both reactions.
- Dimerization and trimerization activation energies were respectively 37 and 89 kJ/mol.

ARTICLE INFO

Article history:
Received 30 May 2013
Received in revised form 30 July 2013
Accepted 18 August 2013
Available online 30 August 2013

Keywords:
Trimerization
Dimerization
Isoamylene
Kinetic
Olefin

ABSTRACT

A kinetic study of the dimerization and the trimerization of isoamylenes (2-methyl-1-butene and 2-methyl-2-butene) in liquid-phase catalyzed by the acidic macroreticular ion exchange resin Amberlyst™ 15 was performed in a continuous-stirred tank reactor in the temperature range 323–393 K using *n*-hexane as a solvent. Reaction rate data were obtained free of internal and external mass transfer resistance effects. The best kinetic models that fit the experimental results were based on the LHHW–ER formalisms. They included the participation of isoamylene, dimer and *n*-hexane in the adsorption term. The number of active sites or clusters implied in the surface reaction was one for dimerization and three for trimerization. It was also inferred that trimers were formed via dimers. Finally, the obtained apparent activation energies for dimerization and trimerization were 37 ± 2 and 89 ± 3 kJ/mol, respectively, being the dimerization activation energy value in agreement with literature data.

1. Introduction

In the last two decades, the comfort and drivability improvement, and especially the fuel tax differentiation, have enhanced the growth of diesel car share in Western European countries. Nowadays, diesel price has increased a lot due to the shortfall in production and it is almost similar to that of gasoline. Owing to the uncertain future trend of fuel consumption, refineries need flexible processes both to supply the variation of gasoline/diesel demand, and to obtain suitable compounds in both blending pools.

On the other hand, volatile organic compounds from evaporative sources are the major contributors of tropospheric ozone generation. As legislation is adopting more stringent specifications of Reid vapor pressure (Rvp) to improve air quality, the consequence is that the lightest components have to be disposed of the gasoline pool. The direct incorporation of bioethanol in fuels would increase the Rvp of the blended fuel. Consequently, it is advisable to produce fuels with lower Rvp to achieve overall fuel specifications. As a result, pentenes and hexenes, which correspond to 40% of volume of the total olefins in gasoline, are in the spotlight to be removed or replaced from gasoline due to their high Rvp [1].

Technologies for upgrading these lighter materials, like C_5/C_6 hydroisomerization, are not appropriate to reduce Rvp [2]. Thus, options to convert C_5/C_6 to heavier compounds and to more suitable components for gasoline and/or diesel are compulsory, not only to satisfy environmental regulations but also to fulfill fuel demand requirements. Among these options, the oligomerization of pentenes over solid acid catalysts has attracted considerable attention [1,3–12], because it allows some flexibility in the gasoline and diesel production.

Pentenes oligomerization is influenced by many factors. Olefin linearity is crucial, since branched olefins are more reactive than lineal olefins due to the higher stability of the tertiary carbocation formed as intermediate compound towards oligomers. Simultaneously, undesirable side reactions, as double bound and skeletal isomerization, cracking to a mixture of intermediate olefins, copolymerizations and hydrogen transfers, can also take place more easily for branched olefins.

* Corresponding author. Tel.: +34 9340221304; fax: +34934021291.
E-mail address: fcunill@ub.edu (F. Cunill).

1385-8947/$ - see front matter © 2013 Elsevier B.V. All rights reserved.
http://dx.doi.org/10.1016/j.cej.2013.08.083

Temperature also plays an important role in this set of reactions. At low temperature, oligomerization, double bound isomerization and skeletal isomerization are the main reactions. At increasing temperature, olefin cracking and disproportionation are promoted, which results in the formation of olefins with intermediate carbon atom number. At higher temperatures, reaction network becomes appreciably more complex because extensive cyclizations and hydrogen transfers involved in the formation of cycloolefins, aromatics, and paraffins take place [13].

The catalyst framework and the olefin length have an important effect on the product distribution due to kinetic and geometric constrains inside the solid catalysts. As a rule of thumb for C_5–C_{14}, the larger the length of alkene is, the lower reactivity to higher oligomers [14]. Indeed, in *n*-hexene and *n*-octene oligomerization performed over zeolites and sulfated zirconias, there were obtained trimers from *n*-hexene but not from *n*-octene [15]. Concerning the selectivity, steric limitations inside the catalysts inhibit the formation of higher oligomers and enhance cracking products formation, because bimolecular oligomerization reactions are more hindered than monomolecular cracking reactions.

For isoamylene oligomerization in absence of alcohols catalyzed by zeolites and ion exchange resins under mild reaction conditions (333–373 K), only diisoamylenes and triisoamylenes were obtained as main products and no significant amounts of higher oligomers were detected [16]. Despite the low temperature, the formation of cracking compounds among C_6–C_9 and C_{11}–C_{14} was also observed. Ion exchange resins showed higher oligomers yields than zeolites, which easily deactivated. A reaction network was proposed in which two possible mechanisms in the trimers formation took place simultaneously: the reaction between three molecules of isoamylenes and the simultaneous reaction of one molecule of dimer with one molecule of isoamylene.

As a result of the great number of compounds present in the reaction mixture and the huge number of different isomers involved, they often cannot be identified and quantified independently. One of the major difficulties for the study of the oligomerization is to propose a reaction scheme and an appropriate kinetic model. In order to simplify this task, all the isomers for each oligomer were lumped together as a single species. It is worth to mention that, even considering oligomerization inhibitor (or moderator) presence such as water and alcohols, literature about kinetics models for olefin oligomerization is quite scarce. In Table 1, working conditions and kinetics results available in the open literature for isobutene and isoamylenes dimerization are summarized. Some authors suggested an Eley–Rideal mechanism (ER) to describe the kinetics of isobutene oligomerization on macroreticular ion exchange resins and zeolites [17,18]. Other authors found more suitable a Langmuir–Hinshelwood–Hougen–Watson mechanism (LHHW) [19,20] or an empirical model with the coexistence of a LHHW mechanism and a modified ER one [21].

With respect to isoamylenes dimerization, it was proposed a first-order kinetic model founded on an Eley–Rideal mechanism in the temperature range 333–373 K by using ion exchange resins as catalyst [22]. On the other hand, by using the macroreticular resin A-35 in the same temperature range with the presence of a 10 mol% of C_1–C_5 alcohols, a LHHW model based on activities was proposed by other authors [6]. In that model, the surface reaction between two adsorbed isoamylene molecules was the rate limiting step, and the number of active sites involve was three. Later, using ethanol as a selectivity enhancer and A-35 as catalyst in a batch reactor with the aim to evaluate the formation of the different dimers and trimers, a LHHW model and a pseudo-homogeneous model were suggested [7]. In this work, it was also proposed that trimers could be simultaneously formed from three molecules of *IA* or from one molecule of *DIA* with one of *IA*. Recently, a screening study of twelve macroreticular ion exchange resin by using the initial isoamylenes reaction rate as a criterion of selection was performed at 343 and 383 K in a batch mode reactor [23]. This work included a preliminary study of the kinetic data, showing that one heterogeneous ER kinetic model was better than two pseudo-homogeneous ones.

To the best of our knowledge, neither studies on isoamylene oligomerization over ion exchange resins in a continuous stirred reactor, nor isoamylene trimerization kinetic studies have been published in the open literature. Therefore, the present work is focused on the kinetic study of the isoamylene oligomerization (particularly in the isoamylene trimerization but also in the dimerization) performed in liquid-phase in a continuous stirred tank in the temperature range 323–393 K over the macroreticular ion exchange resin Amberlyst™ 15 in absence of alcohols. As polar components are not desirable for the study of trimerization because they act as inhibitors of this reaction [6], the two main differences between the present work in front of others with the presence of polar components are the increase of both the isoamylene reaction rates and the trimer selectivity. The option of using a continuous stirred tank reactor is related with the precision and reliability of the experimental reaction rates. Advantages of batch reactor are simplicity and the large number of data point on a time-concentration curve obtained in a single run. The main disadvantage is the calculation of the reaction rates from time-concentration curve, which results in a loss of precision and reliability. In a continuous-stirred reactor, reaction rates can be directly obtained experimentally in the steady state by calculating the difference in concentration between inlet and outlet divided

Table 1
Previous kinetic works about isobutene and isoamylenes dimerization catalyzed by macroreticular resins.

Authors	Reactant	Solvent/inhibitor	Catalyst	Mechanism	E_a (kJ/mol)	REACTOR	Reaction rate values (mmol kg^{-1} s^{-1})
Haag [17]	Isobutene	*n*-C_5, *n*-C_6	Amberlyst 15	ER	77	BATCH, 273 K	9 (r^o_{DIB})
Hauge et al. [18]	Isobutene	*n*-butane	Amberlyst 15	1st order	48	PFR, 313–333 K (WHSV = 1–400 h^{-1})	45–200 ($-r_{IB}$)
Rehfinger and Hoffmann [19]	Isobutene	1-butene	Amberlyst 15	2nd order	40	STCR, 333–363 K	–
Honkela et al. [20]	Isobutene	*n*-pentane/TBA	Amberlyst 15	LHHW *n* = 2	30	STCR, 373 K (WHSV = 36 h^{-1})	50–200 ($-r_{IB}$) 30–60 (r_{DIB}) 0–25 (r_{TRIB})
Izquierdo et al. [21]	Isobutene C_4 SC cut	*n*-butane	Lewatit K-2631	Empirical LH + modified ER	–	BATCH, 323 K	3–60 (r^o_{DIB})
Shah and Sharma [22]	Isoamylene	No solvent	Amberlyst 15	1st order	48.1	BATCH, 333–373 K	–
Cruz et al. [6]	Isoamylene	No solvent, primary alcohols C_1–C_5	Amberlyst 35	LHHW *n* = 3	35–55	BATCH 333–373 K	5–38 (r^o_{DIA})
Cruz et al. [7]	Isoamylene	Ethanol	Amberlyst 35	LHHW *n* = 3	55–65	BATCH 333–373 K	15–160 (r^o_{DIA})
Granollers et al. [23]	Isoamylene	No solvent	Amberlysts Purolites	ER	–	BATCH 343–383 K	13–710 ($-r^o_{IA}$)

by the average residence time under constant conditions. All of this at the expense of obtaining only one data point for each run. Thus, many runs are needed for kinetic studies in a continuous reactor compared with a batch one, but they are much more reliable and precise.

2. Experimental

2.1. Materials

Reactants consisted of an isoamylene mixture of 2-methyl-2-butene (94 wt.%) and 2-methyl-1-butene (6 wt.%) (FLUKA, Germany). As solvent *n*-hexane (FLUKA, Germany) was used because neither reacted with the isoamylenes and products, nor overlapped with other peaks in the chromatogram and it did not inhibit the trimerization. Besides, *n*-hexane had a similar molecular weight and density than reactants and its molecular size is small enough to prevent the blockage of catalyst pores.

The macroreticular ion exchange resin Amberlyst™ 15 (A-15) was used as catalyst. This ion exchange resin was chosen for two reasons. Firstly, A-15 and faujasite zeolite H-FAU-30 were found to be the best catalysts obtained in a previous work for trimerization when was operated in batch mode [16]. Secondly, because studies about isobutene oligomerization in continuous mode showed that resins were more stable to deactivation than zeolites [21,24]. A-15 has an acid capacity of 4.81 eq H^+/kg, a specific surface area obtained by BET method of 42 m^2/g, a pore volume determined by adsorption–desorption of N_2 at 77 K of 0.33 cm^3/g, a mean pore diameter of 31.8 nm, and the mean particle diameter of 0.74 mm. Its skeletal density measured by Helium displacement is 1.42 g/cm^3, its porosity in dry state is 31.7% and the limit working temperature is 393 K.

2.2. Apparatus

All experiments were carried out in a 120-mL stainless steel jacketed autoclave operating in continuous mode. Reaction temperature ranged from 323 K to 393 K, and was controlled within ±1 K by an electric furnace. The reaction took place in liquid phase at 1.5 MPa. Liquid feed (isoamylenes and *n*-hexane) was introduced to the reactor from a 2.5 L vessel equipped with a 100 μm filter placed prior to the pump admission to retain all possible solid feed impurities. At the end of the pipe, products were collected in another 2.5 L vessel. Feed flow rates were controlled by a LabAlliance Series II volumetric pump that supplied a maximum flow rate of 10 mL/min. A Robinson-Mahoney catalytic basket of 0.25 mm of stainless steel mesh was used as catalyst container. The entire process was controlled by a computer with a tailor-made LabVIEW software program.

2.3. Analysis method

Pressurized liquid samples (0.2 μL) were taken out from the reactor outlet by means of a sampling valve (Valco A2CI4WE.2, Switzerland) and injected to GL chromatograph (Agilent 6890N) equipped with a capillary column (TR-120141, TRACSIL TBR-5, 10.0 m × 100 μm × 0.10 μm nominal, Teknokroma, Spain,) and with a flame ionization detector (FID). Helium (Abelló-Linde, Barcelona, Spain), with a minimum purity of 99.998%, was used as carrier gas. Injector temperature was set to 553 K, and FID temperature to 573 K. Oven temperature was programmed with a 1.0 min hold at 313 K, followed by a 75 K/min ramp up to 383 K, maintained for 0.5 min. A second temperature ramp of 50 K/min heated the oven to 423 K; this temperature was hold for 0.8 min.

Due to their similar retention times, chromatographic peaks were lumped in six groups: isoamylenes (*IA*), *n*-hexane (*Hx*), C_6–C_9 cracking products, diisoamylenes (*DIA*), C_{11}–C_{14} cracking products and triisoamylenes (*TIA*). No significant amounts of compounds higher than trimers were detected. So, each group was calibrated by means of an absolute calibration of the compounds that had been previously separated through multiple atmospheric distillations from the reaction products produced in preliminary runs.

2.4. Procedure

The pretreatment of A-15 to remove the moisture consisted of drying at 383 K for 3 h in an atmospheric oven and subsequently, during 5 h at 373 K under vacuum. The residual amount of water was less than 3 wt.% (Karl-Fisher titration). In each experiment, the catalytic basket was loaded with 2 g of fresh dried catalyst. A known amount of reactant mixture (about 120 mL) was introduced in a calibrated burette and the feed vessel was filled with the same isoamylene concentration. The reactor was heated up to the desired reaction temperature. When the operation temperature was reached, the reactive mixture from the burette was shifted into the reactor impelled with nitrogen. Afterwards, the stirring and the volumetric pump were switched on. Liquid samples from the reactor outlet were taken each 30 min until the steady state was observed (when 5 consecutive samples showed differences in chromatographic areas lower than 3%). Usually, the steady state was reached 70–130 min after the start up, depending on the flow rate itself (corresponding 1–3 residence time units).

2.5. Calculations

Isoamylene conversion, selectivity, and reaction rates for dimers, trimers and cracking products grouped as C_6–C_9 and C_{11}–C_{14} were calculated as follows:

$$X_{IA} = \frac{F^o_{IA} - F_{IA}}{F^o_{IA}} \cdot 100 \quad (1)$$

$$r_{j,\ \mathrm{exp}} = \frac{F_j - F^o_j}{W_{CAT}} \quad (2)$$

$$S_{C6-C9} = \frac{r_{IA\rightarrow C6-C9}}{-r_{IA}} \cdot 100 \quad (3)$$

$$S_{DIA} = \frac{2 \cdot r_{DIA}}{-r_{IA}} \cdot 100 \quad (4)$$

$$S_{C11-C14} = \frac{r_{IA\rightarrow C11-C14}}{-r_{IA}} \cdot 100 \quad (5)$$

$$S_{TIA} = \frac{3 \cdot r_{TIA}}{-r_{IA}} \cdot 100 \quad (6)$$

In Eqs. (3) and (5), $r_{IA\rightarrow C_6-C_9}$ and $r_{IA\rightarrow C_{11}-C_{14}}$, respectively, correspond to the reaction rates of cracking compounds expressed as equivalents of *IA*. For kinetic modeling purposes, the reaction rate of cracking compounds were lumped in the term cracking reaction rate, r_{CC}. This reaction rate is also expressed as equivalents of *IA*, and it was calculated as:

$$r_{CC} = r_{IA\rightarrow C_6-C_9} + r_{IA\rightarrow C_{11}-C_{14}} \quad (7)$$

Some experiments were repeated to estimate the experimental error, which was found to be less than 5%. For all experiments the mass balance experimental difference was also less than 5%.

3. Experimental results and discussion

3.1. Previous experiments in batch mode to test the catalytic basket

The catalyst was placed in a Robinson–Mahoney basket. If the basket is overloaded and the stirring is insufficient the contact between reactants and catalyst could be limited and, therefore, the perfectly mixed ideal flow pattern would not be fulfilled. In order to establish the maximum catalyst load in the basket that assure a good contact between the solid and the liquid reactants, some experiments with and without catalytic basket using catalyst loads between 0.5 and 4 g were carried out in batch mode at 353 K. Experimental data showed only negligible differences within the experimental error for catalyst loads up to 2 g. Hence, to avoid the basket influence, 2 g of catalyst were used in continuous mode.

3.2. External and internal mass transfer effects in the steady state

To evaluate external mass transfer resistances, experiments varying the stirring speed from 500 to 900 rpm and returning to 500 rpm were performed at 364 K with a feed flow rate of 2 mL/min. Experimental data showed no significant external mass transfer resistance under these conditions. In addition, the catalytic activity did not decay after 11 h of run under those conditions. As that experiment were the longest in time on stream terms, it was assumed that the catalyst would not deactivated in the steady state results obtained for the rest of experiments.

Concerning the internal mass transfer resistance, experiments at 364 K and for 1 mL/min of isoamylenes flow rate, and using six different particle size ranging between 0.25 and 1 mm were carried out. For the essayed particles sizes, only differences of the same order of the experimental error were observed and, therefore, it was assumed that internal mass transfer influence was negligible. In subsequent runs, particles sizes of 0.56–0.63 mm were used.

3.3. Effect of the feed flow rate

Space velocity, typically referred to as weight hourly space velocity (WHSV), affects conversion and selectivity. An excessive contact time can allow additional undesirable reactions. With the purpose to study the feed flow rate influence, experiments between 18 and 103 h^{-1} of WHSV, at 364 K and 500 rpm were carried out. All experiments in this WHSV range reached the steady state after 1–3 space times. By comparing the isoamylene conversion and selectivity in the steady state for different WHSV (Fig. 1), it was noticed that the influence of WHSV on selectivity was not significant. Similar results were reported by Yoon et al. [24] when they studied the effect of WHSV among 10–100 h^{-1} on isobutene trimerization. They did not observe any important influence on selectivity for WHSV higher than 25 h^{-1}. Regarding to the isoamylene conversion, it decreased from 80% to 50% due to the reduction of the average residence time, as expected. As the isoamylenes conversion decreased when feed flow rate increased, the concentrations of isoamylenes in the reactor were higher, and subsequently, the reaction rate increased.

As selectivity was not affected by the flow rate it was decided to operate at WHSV equal to 35 h^{-1} (1.6 mL/min) because it was in the optimal working range of the pump and it allowed a higher sensitivity of reactant consumptions and reaction rates.

3.4. Effect of the isoamylene concentration and temperature

A set of experiments were carried out in order to evaluate the effect of the isoamylene concentration and temperature on conversion, selectivity and reaction rates. As diluent, *n*-hexane was used.

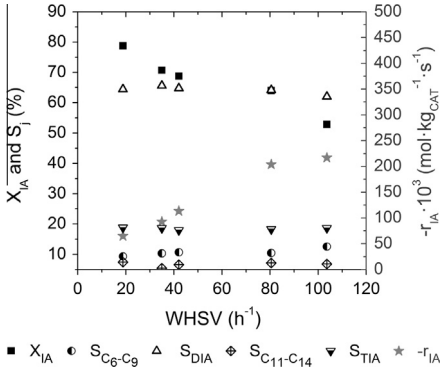

Fig. 1. WHSV influence (2 g A-15, 500 rpm, D_p = 0.56–0.63 mm, 364 K) on isoamylene conversion and reaction rate, and on products selectivities.

Reactor feeds consisted of isoamylene-hexane mixtures with isoamylene content between 25% and 100% (wt.%) and a total flow rate of 1.6 mL/min. Assayed temperatures were in the range 327–384 K and catalyst load was 2 g of Amberlyst™ 15 with 0.56–0.63 mm of particle diameter. Results are shown in Table 2, where it can be observed that selectivity towards products was practically independent of isoamylene concentration and the only influence on selectivity was due to the temperature. On increasing temperature from 327 to 384 K, selectivity towards dimers reduces from 90% to 60%, while selectivity towards trimers and cracking compounds increased roughly from 10% to 20%, and from 0% to 10%, respectively. Table 2 also shows that generally isoamylene conversion, reaction rates of isoamylenes consumption, and those of dimer formation and trimers formation increase with the fed isoamylene concentration and the reactor temperature. Only at the highest temperature, 384 K, dimers formation decreases compared to 364 K, what can be explained by the faster formation of trimers and/or cracking compounds.

Obtained reactions rates (Table 2) can be compared with those obtained in previous works for isobutene and isoamylenes dimerization and for isobutene trimerization catalyzed by acidic macroreticular ion exchange resins (Table 1). As it can be seen, isoamylenes dimerization reaction rates obtained in present work (14–127 mmol/kg s) are in the range of the published data in literature (1–160 mmol/kg s). In addition, trimerization reaction rates are similar to those obtained for isobutene trimerization. This fact reinforces the validity of the obtained results for the trimerization data for which there are no literature data to be compared. Finally, in order to check both the molar balance and the importance of the cracking compounds, experimental isoamylene consumption rates and product formation rates were compared. A good agreement between the consumption and formation rates was evident when cracking formation rates were taken into account (not showed in the text), since differences were lower than 3.2%. Without considering cracking formation rates, at temperatures higher than 353 K, differences up to 20% were observed. As a result, cracking formation was taken into account in the kinetic modeling.

3.5. Derivation of kinetic models

The results of preliminary runs indicated that measured reaction rates were free of mass transfer resistance influences. Besides, it was checked if the reaction mixture behaved ideally. Activity coefficients calculated by means of the Dortmund-modified UNIFAC method [25] were practically equal to unity for all components under all assayed conditions. Consequently, the system can be considered as practically ideal and, therefore, kinetic models can be expressed in terms of concentrations. The reactions to be modeled

Table 2
Selectivity, *IA* conversion and reaction rates for different temperatures and *IA* concentrations (WHSV = 30–35 h^{-1}).

T (K)	*IA* (wt.%)	$F^0 \cdot 10^6$ (kg s^{-1})	S_{C6-C9} (%)	S_{DIA} (%)	$S_{C11-C14}$ (%)	S_{TIA} (%)	X_{IA} (%)	$-r_{IA} \cdot 10^3$ (mol kg^{-1} s^{-1})	$r_{DIA} \cdot 10^3$ (mol kg^{-1} s^{-1})	$r_{TIA} \cdot 10^3$(mol kg^{-1} s^{-1})
327	0.25	16.5	0.6	87.5	0.8	11.3	34.4	32.7	14.3	1.2
	0.50	18.7	0.6	87.4	0.8	11.2	44.9	98.13	42.8	3.7
	0.75	17.5	0.5	87.3	0.8	11.4	47.5	153.1	66.8	5.8
	1.00	13.8	0.6	87.6	0.9	10.9	52.2	185.3	81.2	6.7
344	0.25	16.7	2.8	80.5	3.0	13.7	48.3	48.0	19.3	2.2
	0.50	18.1	3.1	80.1	3.2	13.6	62.1	142.8	57.2	6.5
	0.75	18.0	3.1	81.0	2.9	13.0	64.7	217.0	87.9	9.5
	1.00	18.4	2.9	80.8	3.1	13.2	66.9	315.8	127.5	13.9
364	0.25	17.6	5.9	70.6	6.8	16.7	61.6	65.4	23.1	3.6
	0.30	18.9	5.7	71.0	6.6	16.7	66.0	94.9	33.7	5.3
	0.40	19.2	5.8	71.5	6.5	16.2	67.8	123.1	44.0	6.6
	0.50	17.4	5.6	71.8	6.3	16.3	70.3	153.8	55.2	8.4
	0.75	18.4	5.5	71.5	6.1	16.9	71.4	249.1	89.0	14.0
	1.00	18.8	5.5	71.7	6.2	16.6	73.5	355.5	127.5	19.7
384	0.25	18.7	8.4	61.2	10.4	20.1	68.8	77.1	23.6	5.2
	0.50	18.2	8.8	59.4	10.6	21.2	76.0	170.7	50.7	12.1
	0.75	18.5	8.3	61.1	10.3	20.3	76.5	265.8	81.2	18.0
	1.00	18.3	8.7	59.9	10.9	20.5	78.2	364.4	109.1	24.9

were the dimer and the trimer formation. For the proposal of the plausible models, the following premises were assumed:

(1) Trimers could be formed through two possible mechanisms: firstly, via one isoamylene with one formed dimer (*IA* + *DIA*) and, secondly, from directly three isoamylenes (3IA). The consideration of the second mechanism was based on the controversial proposal existing in literature for isobutene oligomerization. While Honkela et al. [20] proposed to reject trimer formation from three isobutene molecules, Haag [17] proposed both reactions to occur simultaneously. As there were no references about isoamylene trimerization, it was decided to check both possibilities. Therefore, if trimers were considered to come from 3 isoamylenes, the faster consumption of dimers at higher temperature would be associated to the cracking formation according the following scheme:

$$2\mathrm{IA} \rightarrow DIA \quad r_1$$
$$3\mathrm{IA} \rightarrow TIA \quad r_2$$
$$DIA \rightarrow 2\mathrm{CC} \quad r_3$$

Then, formation rates of dimerization (r_1), trimerization (r_2), and dimers cracking (CC), (r_3), would be calculated from experimental compound reaction rates (Eq. (2) to Eq. (7)) as:

$$r_{DIA}(eq.2) = r_1 - r_3 = r_1 - \frac{r_{CC}}{2} \quad \rightarrow \quad r_1 = r_{DIA} + \frac{r_{CC}}{2} \tag{8}$$

$$r_{TIA}(eq.2) = r_2 \quad \rightarrow \quad r_2 = r_{TIA} \tag{9}$$

$$r_{CC}(eq.7) = 2 \cdot r_3 \quad \rightarrow \quad r_3 = \frac{r_{CC}}{2} \tag{10}$$

If trimerization was considered to proceed via dimers, firstly a faster consumption of dimers at higher temperature would be associated to the formation of trimers and, secondly trimers which are the largest molecules could be easily cracked as:

$$2\mathrm{IA} \rightarrow DIA \quad r_1$$
$$DIA + \mathrm{IA} \rightarrow TIA \quad r_2$$
$$TIA \rightarrow 3\mathrm{CC} \quad r_3$$

In that case, the reaction rate for each reaction could be obtained from the experimental compositions (Eq. (2) to Eq. (7)) according to:

$$r_{DIA}(eq.2) = r_1 - r_2 \quad \rightarrow \quad r_1 = r_{DIA} + r_2 \quad \rightarrow \quad r_1 = r_{DIA} + r_{TIA} + \frac{r_{CC}}{3} \tag{11}$$

$$r_{TIA}(eq.2) = r_2 - r_3 = r_2 - \frac{r_{CC}}{3} \quad \rightarrow \quad r_2 = r_{TIA} + \frac{r_{CC}}{3} \tag{12}$$

$$r_{CC}(eq.7) = 3 \cdot r_3 \quad \rightarrow \quad r_3 = \frac{r_{CC}}{3} \tag{13}$$

(2) To limit the number of models to be checked, the maximum number of active centers or clusters of active centers (multicenter adsorption or multiplet of sulfonic groups), considered to be involved in the rate-determining step, is three. An active center can be formed by only one sulfonic group or by a cluster of them. The number of sulfonic groups that form a cluster would depend on the resin and on the reacting medium. In a non-polar medium where the sulfonic groups are not disaggregated, it is expected a cluster formed by several sulfonic groups. This assumption should be taken into account to interpret the exponent of the adsorption term.

(3) All reactions are irreversible and their reaction rate is supposed to follow hyperbolic kinetic models based on Langmuir–Hinshelwood–Hougen–Watson (LHHW) and Eley–Rideal (ER) mechanisms.

(4) For both two mechanisms, the surface reaction is assumed to be the rate-limiting step of each reaction [7], and the steps of adsorption–desorption of the isoamylene, dimer, trimer and hexane are at equilibrium. It is assumed that the adsorption of each molecule takes place on one active center.

According to the previous assumptions the following mechanisms can be proposed, where the adsorption–reaction–desorption equilibrium steps have been omitted:

MECHANISM 1: Dimers from 2 isoamylenes and trimers from 3 isoamylenes (LHHW or ER):

$$\text{Dimerization}: \quad 2IA\sigma + (\mathrm{n}-2)\sigma \rightarrow DIA\sigma + (\mathrm{n}-1)\sigma \quad (\mathrm{D_{LHHW}})$$
$$\text{or}$$
$$IA\sigma + IA + (\mathrm{n}-1)\sigma \rightarrow DIA\sigma + (\mathrm{n}-1)\sigma \quad (\mathrm{D_{ER}})$$

$$\text{Trimerization}: \quad 3IA\sigma \rightarrow TIA\sigma + 2\sigma \quad (\mathrm{T_{LHHW,3}}IA)$$
$$\text{or}$$
$$IA\sigma + 2IA + (\mathrm{n}-1)\sigma \rightarrow TIA\sigma + (\mathrm{n}-1)\sigma \quad (\mathrm{T_{ER-1,3}}IA)$$
$$\text{or}$$
$$2IA\sigma + IA + (\mathrm{n}-2)\sigma \rightarrow TIA\sigma + (\mathrm{n}-1)\sigma \quad (\mathrm{T_{ER-2,3}}IA)$$

MECHANISM 2: Dimers from 2 isoamylenes and trimers from one dimer molecule with one isoamylene molecule (LHHW or ER):

Dimerization: $2IA\sigma + (n-2)\sigma \rightarrow DIA\sigma + (n-1)\sigma$ (D_{LHHW})
or
$IA\sigma + IA + (n-1)\sigma \rightarrow DIA\sigma + (n-1)\sigma$ (D_{ER})

Trimerization: $IA\sigma + DIA\sigma + (n-2)\sigma \rightarrow TIA\sigma + (n-1)\sigma$ ($T_{LHHW,DIA+IA}$)
or
$IA\sigma + DIA + (n-1)\sigma \rightarrow TIA\sigma + (n-1)\sigma$ ($T_{ER-I,DIA+IA}$)
or
$IA + DIA\sigma + (n-1)\sigma \rightarrow TIA\sigma + (n-1)\sigma$ ($T_{ER-D,DIA+IA}$)

As the surface reaction is assumed to be the rate-limiting step, the following LHHW kinetic expressions are derived:

$$r_{1,calc} = \frac{\hat{k}_1 \cdot K_{IA}^2 \cdot c_{IA}^2}{(1 + K_{IA} \cdot c_{IA} + K_{DIA} \cdot c_{DIA} + K_{TIA} \cdot c_{TIA} + K_{Hx} \cdot c_{Hx})^n} \quad (D_{LHHW}) \quad (14)$$

$$r_{2,calc} = \frac{\hat{k}_2 \cdot K_{IA}^3 \cdot c_{IA}^3}{(1 + K_{IA} \cdot c_{IA} + K_{DIA} \cdot c_{DIA} + K_{TIA} \cdot c_{TIA} + K_{Hx} \cdot c_{Hx})^n} \quad (T_{LHHW,3IA}) \quad (15)$$

$$r_{2,calc} = \frac{\hat{k}_2 \cdot K_{IA} \cdot K_{DIA} \cdot c_{IA} \cdot c_{DIA}}{(1 + K_{IA} \cdot c_{IA} + K_{DIA} \cdot c_{DIA} + K_{TIA} \cdot c_{TIA} + K_{Hx} \cdot c_{Hx})^n} \quad (T_{LHHW,DIA+IA}) \quad (16)$$

And for ER formalism:

$$r_{1,calc} = \frac{\hat{k}_1 \cdot K_{IA} \cdot c_{IA}^2}{(1 + K_{IA} \cdot c_{IA} + K_{DIA} \cdot c_{DIA} + K_{TIA} \cdot c_{TIA} + K_{Hx} \cdot c_{Hx})^n} \quad (D_{ER}) \quad (17)$$

$$r_{2,calc} = \frac{\hat{k}_2 \cdot K_{IA} \cdot c_{IA}^3}{(1 + K_{IA} \cdot c_{IA} + K_{DIA} \cdot c_{DIA} + K_{TIA} \cdot c_{TIA} + K_{Hx} \cdot c_{Hx})^n} \quad (T_{ER-1,3IA}) \quad (18)$$

$$r_{2,calc} = \frac{\hat{k}_2 \cdot K_{IA}^2 \cdot c_{IA}^3}{(1 + K_{IA} \cdot c_{IA} + K_{DIA} \cdot c_{DIA} + K_{TIA} \cdot c_{TIA} + K_{Hx} \cdot c_{Hx})^n} \quad (T_{ER-2,3IA}) \quad (19)$$

$$r_{2,calc} = \frac{\hat{k}_2 \cdot K_{IA} \cdot c_{IA} \cdot c_{DIA}}{(1 + K_{IA} \cdot c_{IA} + K_{DIA} \cdot c_{DIA} + K_{TIA} \cdot c_{TIA} + K_{Hx} \cdot c_{Hx})^n} \quad (T_{ER-I,DIA+IA}) \quad (20)$$

$$r_{2,calc} = \frac{\hat{k}_2 \cdot K_{DIA} \cdot c_{IA} \cdot c_{DIA}}{(1 + K_{IA} \cdot c_{IA} + K_{DIA} \cdot c_{DIA} + K_{TIA} \cdot c_{TIA} + K_{Hx} \cdot c_{Hx})^n} \quad (T_{ER-D,DIA+IA}) \quad (21)$$

The surface rate constant, $\hat{k}$, and the adsorption equilibrium constants, K_{IA} and K_{DIA}, were grouped into factors k'_1 and k'_2. By this way, LHHW and ER based equations for dimerization and trimerization reaction rates are mathematically equivalent. Then, the following general models for dimerization and trimerization were obtained:

$$r_{1,calc} = \frac{k'_1 \cdot c_{IA}^2}{(1 + K_{IA} \cdot c_{IA} + K_{DIA} \cdot c_{DIA} + K_{TIA} \cdot c_{TIA} + K_{Hx} \cdot c_{Hx})^n} \quad (D) \quad (22)$$

$$r_{2,calc} = \frac{k'_2 \cdot c_{IA}^3}{(1 + K_{IA} \cdot c_{IA} + K_{DIA} \cdot c_{DIA} + K_{TIA} \cdot c_{TIA} + K_{Hx} \cdot c_{Hx})^n} \quad (3I) \quad (23)$$

$$r_{2,calc} = \frac{k'_2 \cdot c_{IA} \cdot c_{DIA}}{(1 + K_{IA} \cdot c_{IA} + K_{DIA} \cdot c_{DIA} + K_{TIA} \cdot c_{TIA} + K_{Hx} \cdot c_{Hx})^n} \quad (D + I) \quad (24)$$

On the basis of these equations, all possible kinetic models derived by considering one or more components of adsorption term being negligible were fitted to the experimental reaction rate data. The adsorption term of hexane has been included because, for low initial concentrations of IA, the hexane concentration is high and its contribution in the adsorption term could be significant. All models were grouped in two classes, as showed in Table 3:

(i) Class I, for which the number of free active centers is considered to be negligible compared to occupied ones. This fact implies that the unity present in the adsorption term is removed, because it is small compared with the rest of the others adsorption terms.
(ii) Class II, for the opposite case.

In Table 3 the variable P stands for the driving force: c_{IA}^2 in the case of dimerization, c_{IA}^3 in the case of trimerization via 3IA, and $c_{IA} \cdot c_{DIA}$ in the case of trimerization via *DIA + IA*. In Class I, parameter A is related to the kinetic constant and parameters B to G to adsorption equilibrium constants for mathematical fitting purposes. The temperature dependence of such factors and of the apparent kinetic constants k'_1 and k'_2 were defined as follows according to the Arrhenius law:

$$k', A, B, C, D, E, F, G = \exp(M_i) \exp\left[-N_i\left(\frac{1}{T} - \frac{1}{\bar{T}}\right)\right] \quad (25)$$

where $\bar{T}$ was the mean experimental temperature and the subscript i denotes the adjusted parameter. The subtraction of the inverse of the mean experimental temperature was included to minimize correlations among fitted parameters M_i and N_i .

A set of optimal parameter values was obtained for each model that minimized the sum of squares of residuals between experimental rates, considering Eqs. (8)–(13) when appropriated, and

Table 3
Kinetic equations proposed for dimerization ($P = c_{IA}^2$), trimerization via 3IA ($P = c_{IA}^3$) and trimerization via *DIA + IA* ($P = c_{IA} \cdot c_{DIA}$). $B = K_{DIA} \cdot K_{IA}^{-1}$, $C = K_{TIA} \cdot K_{IA}^{-1}$, $D = K_{Hx} \cdot K_{IA}^{-1}$, $E = K_{TIA} \cdot K_{DIA}^{-1}$, $F = K_{Hx} \cdot K_{DIA}^{-1}$, and $G = K_{Hx} \cdot K_{TIA}^{-1}$. Assayed values for n where 1, 2, and 3.

Type	Models class I	Models class II
0		$r_{calc} = k'\,P$
1	$r_{calc} = A\frac{P}{c_{IA}^n}$	$r_{calc} = \frac{k'P}{(1+K_{IA}\,c_{IA})^n}$
2	$r_{calc} = A\frac{P}{c_{DIA}^n}$	$r_{calc} = \frac{k'\,P}{(1+K_{DIA}\,c_{DIA})^n}$
3	$r_{calc} = A\frac{P}{c_{TIA}^n}$	$r_{calc} = \frac{k'P}{(1+K_{TIA}\,c_{TIA})^n}$
4	$r_{calc} = A\frac{P}{c_{Hx}^n}$	$r_{calc} = \frac{k'\,P}{(1+K_{Hx}\,c_{Hx})^n}$
5	$r_{calc} = \frac{A\,P}{(c_{IA}+B\,c_{DIA})^n}$	$r_{calc} = \frac{k'\,P}{(1+K_{IA}\,c_{IA}+K_{DIA}\,c_{DIA})^n}$
6	$r_{calc} = \frac{A\,P}{(c_{IA}+C\,c_{TIA})^n}$	$r_{calc} = \frac{k'\,P}{(1+K_{IA}\,c_{IA}+K_{TIA}\,c_{TIA})^n}$
7	$r_{calc} = \frac{A\,P}{(c_{IA}+D\,c_{Hx})^n}$	$r_{calc} = \frac{k'\,P}{(1+K_{IA}\,c_{IA}+K_{Hx}\,c_{Hx})^n}$
8	$r_{calc} = \frac{A\,P}{(c_{DIA}+E\,c_{TIA})^n}$	$r_{calc} = \frac{k'\,P}{(1+K_{DIA}\,c_{DIA}+K_{TIA}\,c_{TIA})^n}$
9	$r_{calc} = \frac{A\,P}{(c_{DIA}+F\,c_{Hx})^n}$	$r_{calc} = \frac{k'\,P}{(1+K_{DIA}\,c_{DIA}+K_{Hx}\,c_{Hx})^n}$
10	$r_{calc} = \frac{A\,P}{(c_{TIA}+G\,c_{Hx})^n}$	$r_{calc} = \frac{k'\,P}{(1+K_{TIA}\,c_{TIA}+K_{Hx}\,c_{Hx})^n}$
11	$r_{calc} = \frac{A\,P}{(c_{IA}+B\,c_{DIA}+C\,c_{TIA})^n}$	$r_{calc} = \frac{k'\,P}{(1+K_{IA}\,c_{IA}+K_{DIA}\,c_{DIA}+K_{TIA}\,c_{TIA})^n}$
12	$r_{calc} = \frac{A\,P}{(c_{IA}+B\,c_{DIA}+D\,c_{Hx})^n}$	$r_{calc} = \frac{k\,P}{(1+K_{IA}\,c_{IA}+K_{DIA}\,c_{DIA}+K_{Hx}\,c_{Hx})^n}$
13	$r_{calc} = \frac{A\,P}{(c_{IA}+C\,c_{TIA}+D\,c_{Hx})^n}$	$r_{calc} = \frac{k'\,P}{(1+K_{IA}\,c_{IA}+K_{TIA}\,c_{TIA}+K_{Hx}\,c_{Hx})^n}$
14	$r_{calc} = \frac{A\,P}{(c_{DIA}+E\,c_{TIA}+F\,c_{Hx})^n}$	$r_{calc} = \frac{k'\,P}{(1+K_{DIA}\,c_{DIA}+K_{TIA}\,c_{TIA}+K_{Hx}\,c_{Hx})^n}$
15	$r_{calc} = \frac{A\,P}{(c_{IA}+B\,c_{DIA}+C\,c_{TIA}+D\,c_{Hx})^n}$	$r_{calc} = \frac{k'\,P}{(1+K_{IA}\,c_{IA}+K_{DIA}\,c_{DIA}+K_{TIA}\,c_{TIA}+K_{Hx}\,c_{Hx})^n}$

calculated rates from models of Table 3 by using Marquardt–Levenberg method [26].

From a mathematical point of view, the most suitable model is the one for which the minimum sum of squared residuals (SSR), residuals randomness, and lower parameter correlation are obtained with the minimum number of fitted parameters. On the other hand, parameters of the best model should have a physicochemical meaning, i.e. rate constant, and adsorption equilibrium constants, must increase, and decrease, respectively, with temperature, because reaction activation energy has to be positive and adsorption enthalpies negative.

To make comparisons among goodness of fit for different models a relative SSR has been defined as the ratio SSR_{min}/SSR.

3.6. Kinetic modeling results

Relative SSR for trimerization which fulfills the physicochemical premises are compared in Fig. 2, where the model with the best mathematical fit presents a maximum value of relative SSR equal to unity. Fig. 2A depicts SSR_{min}/SSR for the different proposed trimerization models of Class I and Class II when trimers are considered to come from three isoamylenes (Mechanism 1), and Fig. 2B when they are supposed to take place via *DIA* + *IA* (Mechanism 2). As a whole, models via dimer mechanism (Mechanism 2) predict better the trimer formation reaction rate than models via 3IA mechanism. It was also observed that, in general, Class I models provided better fit for both mathematical and thermodynamic consistency criteria than Class II models. In addition, models with $n = 3$ fitted the experimental data better than for $n = 2$ for both classes. The worst fits were obtained for $n = 1$. Then, from Fig. 2 it is deduced that the bests models were Class I models 12, 14 and 15 for $n = 3$ through mechanism 2.

In accordance with the mechanism 2, dimerization modeling was performed then using the dimerization formation rate calculated with Eq. (11). In Fig. 3, models with thermodynamic consistency are compared for dimerization by means of SSR_{min}/SSR. It can be seen again that Class I models showed more thermodynamic consistency than Class II. Among the best models of Class I, the best fit was obtained for $n = 1$ and the worst for $n = 3$. Therefore, the best models for dimerization were Class I models 7, 12, 13 and 15 for $n = 1$. As models 12 and 15 were also the best ones in trimerization and showed the best fit, these two models were further considered.

For dimerization and trimerization, comparing models 12 and 15, the only difference was the trimer presence in the adsorption term, $C{\cdot}c_{TIA}$. However, the results of the fit of model 15 showed a value of trimer adsorption contribution term, $C{\cdot}c_{TIA}$, lower by far than for the rest of adsorption terms for both reactions (for dimerization 10^{-19} and for trimerization 10^{-34}) and, therefore, this term could be neglected. As a consequence, model 12 and 15 coincided, and the best fit is obtained with the following equations:

$$\text{Dimer formation}: \quad r_1 = \frac{A_1\, c_{IA}^2}{(c_{IA} + B c_{DIA} + D\, c_{Hx})}$$

and

$$\text{Trimer formation}: \quad r_2 = \frac{A_2\, c_{IA} c_{DIA}}{(c_{IA} + B c_{DIA} + D c_{Hx})^3}$$

where

$$A_1 = \frac{k_1'}{K_{IA}}$$

$$A_2 = \frac{k_2'}{K_{IA}^3}$$

$$B = \frac{K_{DIA}}{K_{IA}}$$

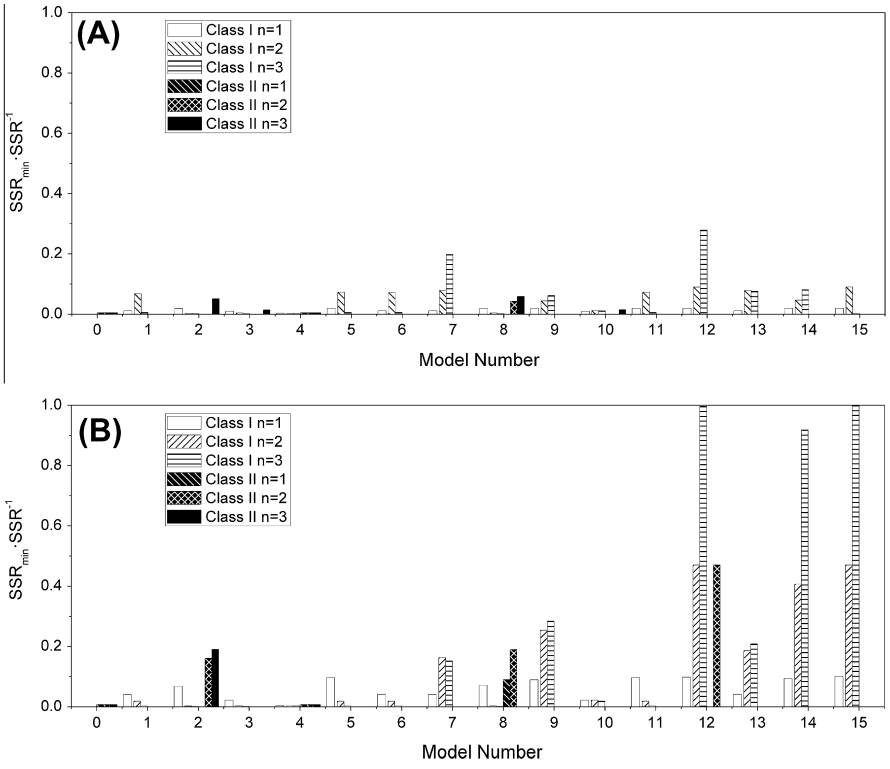

Fig. 2. Comparison of the goodness of fit of class I and class II in terms of SSR_{min}/SSR for trimerization reaction: (A) via 3IA; (B) via *DIA* + *IA*. The best fit corresponds to the maximum SSR_{min}/SSR value, equal to unity.

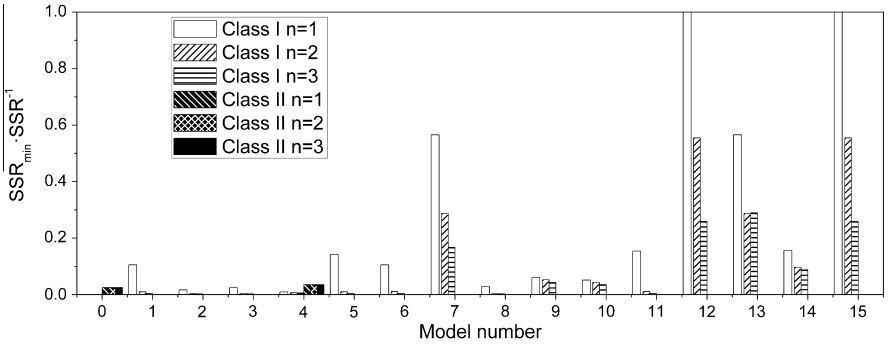

Fig. 3. Comparison of the goodness of fit of class I and class II in terms of SSR_{min}/SSR for dimerization reaction. The best fit corresponds to the maximum SSR_{min}/SSR value, equal to unity.

and

$$D = \frac{K_{Hx}}{K_{IA}}$$

The fitted parameters values of these equations with their confidence interval at 95% obtained by Jackknife method are presented in Table 4. It is interesting to notice the similarities between the adsorption parameter values from dimerization and trimerization equations, even with the high confidence interval and the nonlinear independent fit. For both equations, correlations among parameters were computed using the correlation matrix (Table 5). As all the non-diagonal values of the matrix were lower than 0.48, it was assumed that there were no significant correlations. To complete the evaluation of the goodness-of-fit, the calculated reactions rates versus the experimental formation rates (Figs. 4A and 5A), and the residuals respect these experimental reaction rates (Figs. 4B and 5B) are depicted in Figs. 4 and 5 for dimerization and trimerization reactions, respectively. It was obtained a good prediction of the experimental values and randomness of residuals. As both kinetic equations showed to be suitable from mathematical point of view, they can be used to infer the possible mechanism of reaction, and to calculate the kinetic parameters of activation energy, enthalpy of adsorption, and entropy of adsorption.

According to selected kinetic equations, significant adsorption terms are the adsorption of isoamylenes, dimers and hexane.

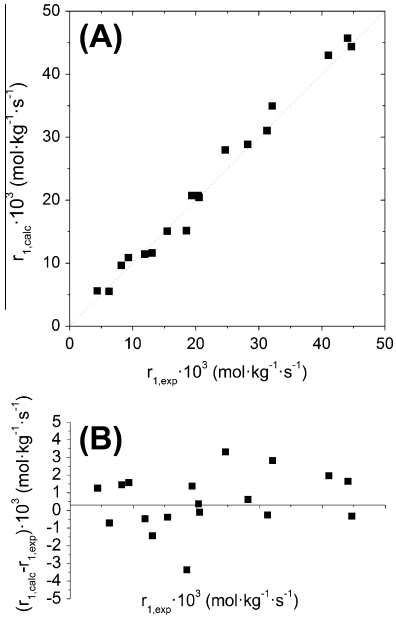

Fig. 4. Statistical analysis of dimerization resultant kinetic equation: (A) Calculated reaction correspondence; (B) Randomness of residuals.

Table 4
Parameters for dimerization and trimerization kinetic equations with a confidence interval of 95%.

		Dimerization	Trimerization
Kinetic constant, A	M_1	3.97 ± 0.25	8.9 ± 0.61
	N_1	4435 ± 249	10,667 ± 392
Adsorption term $B = K_{DIA} \cdot K_{IA}^{-1}$	M_2	2.20 ± 0.18	1.50 ± 0.26
	N_2	1615 ± 371	1874 ± 388
Adsorption term $D = K_{Hx} \cdot K_{IA}^{-1}$	M_3	−2.53 ± 0.11	−0.12 ± 0.22
	N_3	2534 ± 549	2752 ± 510

Isoamylenes and diisoamylenes were involved as reactants and products in the oligomerization reaction, so it was not surprising their contribution in the adsorption term. Although hexane is inert, its effect on kinetics could be explained due to its interaction with the resin matrix, what could modify the acid centers conformation.

Mechanism 2 explained better the dimerization and trimerization formation rates. In the case of dimerization with the participation of one active site or cluster of active sites, the most plausible mechanism for dimerization is based on a Eley–Rideal mechanism. So, the reaction takes place between one adsorbed isoamylene molecule on the surface with a free isoamylene. For trimers, it

Table 5
Correlation matrix of the fitted parameters for dimerization and trimerization reactions.

Reaction	Dimerization						Trimerization					
Parameter	M_1	N_1	M_2	N_2	M_3	N_3	M_1	N_1	M_2	N_2	M_3	N_3
M_1	1	0.48	0.35	−0.26	0.34	0.13	1	−0.09	0.32	0.19	−0.17	−0.32
N_1	0.48	1	0.43	0.31	−0.12	0.42	−0.09	1	−0.03	−0.06	0.08	0.22
M_2	0.35	0.43	1	−0.38	−0.40	0.10	0.32	−0.03	1	0.04	−0.01	−0.07
N_2	−0.26	0.31	−0.38	1	0.20	−0.01	0.19	−0.06	0.04	1	−0.04	−0.11
M_3	0.34	−0.12	−0.40	0.20	1	−0.31	−0.17	0.08	−0.01	−0.04	1	−0.32
N_3	0.13	0.42	0.10	−0.01	−0.31	1	−0.32	0.22	−0.07	−0.11	−0.32	1

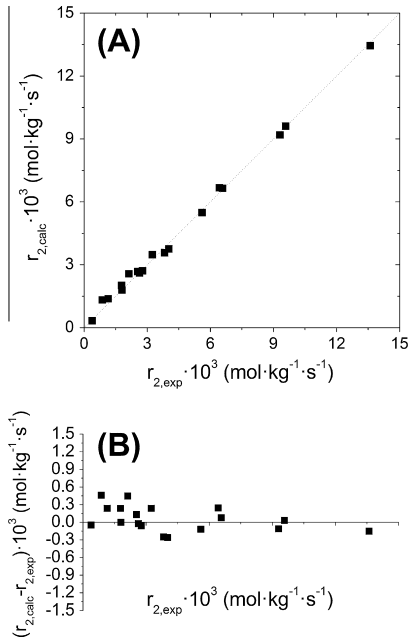

Fig. 5. Statistical analysis of trimerization resultant kinetic equation: (A) Calculated reaction correspondence; (B) Randomness of residuals.

can be inferred that their formation take place as a consecutive reaction to dimerization. Notwithstanding, the kinetic equation does not provide information about which compound or compounds are adsorbed in the catalytic surface. The only information provided is the number of active sites or clusters involved in the reaction, which is equal to 3. The increase from one to three active sites or clusters from dimerization to trimerization could be explained by means of stabilization of the intermediate. Dimers are more branched and larger than isoamylenes and they could need an extra active site or cluster alongside to accommodate the reaction of trimerization. In fact, one of the conclusions of a previous work in batch mode over different ion exchange resins [23], was that trimerization mainly occur in the inner zone of the gel-phase of ion exchange resins, because of the higher probability to obtain the adequate spatial conformation and acid density.

The last part of the kinetic study involved the calculation and interpretation of the kinetic parameters for both formation reactions. Apparent activation energies for dimerization and trimerization were obtained from variation of the kinetic parameters A_1 and A_2 with temperature, resulting in values of 37 ± 2 kJ/mol and 89 ± 3 kJ/mol, respectively (Table 6). Apparent activation energy for dimerization reaction was in the range of the values given in the literature as seen in Table 1. Therefore, it was considered consistent and reliable. The estimated value of activation energy for trimerization was higher than for dimerization. Due to the lack of data available in the literature, this value cannot be corroborated. The large difference in the activation energy of dimerization and trimerization can be attributed to the higher energy barrier to overcome the transition state from dimers to trimers compared to that obtained for dimerization from isoamylenes. In addition, steric impediments are more important in trimerization and they could be more sensitive to temperature, which results in a larger activation energy.

Finally, it was studied the adsorption enthalpy and entropy of the species involved in the kinetic equation. Because of the chosen kinetic models, adsorption enthalpies and entropies cannot be estimated independently for diisoamylenes, amylenes and 1-hexane from fitted parameters B and D, since they give only differences. In Table 6, the differences of enthalpy and entropy of dimers versus isoamylene and hexane versus isoamylenes are summarized. From the values of difference of adsorption enthalpy, it can be concluded that the increment of enthalpy of adsorption of hexane and dimer are higher than that of isoamylenes. On the other hand, the increment of adsorption entropy resulted higher for dimer than for isoamylene, but was lower for hexane than for isoamylenes. By using Eq. (25) with parameter values of Table 4 it results that the diisoamylene adsorption equilibrium constant is higher than that of isoamylene, which is in agreement with previous published data [6], and with the recently published values for oligomerization of α-olefins over A-15 [14]. Besides, the adsorption equilibrium constant for isoamylene is higher than that for 1-hexene.

It is to bear in mind that the proposed mechanism of reaction based only on kinetic analysis and without spectroscopy base is only a potential possible mechanism, and it acquires somehow the category of empirical mechanism without becoming it.

Table 6
Apparent activation energies for dimerization and differences of adsorption enthalpy and entropy between dimers and isoamylenes and hexane versus isoamylene with a confidence interval of 95%.

Reaction fitted	E_a (kJ mol^{-1})	$\Delta H_{DIA}-\Delta H_{IA}$ (kJ mol^{-1})	$\Delta H_{Hx}-\Delta H_{IA}$ (kJ mol^{-1})	$\Delta S_{DIA}-\Delta S_{IA}$ (J K^{-1} mol^{-1})	$\Delta S_{Hx}-\Delta S_{IA}$ (J K^{-1} mol^{-1})
Dimerization	37 ± 2	13 ± 3	21 ± 5	18 ± 1	−21 ± 1
Trimerization	89 ± 3	15 ± 3	23 ± 4	12 ± 2	−1 ± 2

4. Conclusions

No significant external or internal mass transfer resistances were observed for the stirring speed range of 500–900 rpm and bead sizes lower than 0.56–0.63 mm fraction. There is no influence on selectivity with WHSV in the range of 18–103 h^{-1} and for isoamylenes mass fractions between 25% and 100% (w/w). When temperature increased, the selectivity toward dimers decreased, and that toward trimers and cracking products, increased from 10% to 20%, and from 0% to 10%, respectively.

In dimerization and trimerization modeling were proposed two mechanisms to produce trimers. The second mechanism with the formation of trimers by the addition of one isoamylene molecule to one dimer molecule showed to explain better the formation reaction rates obtained. From this mechanism, kinetic equations that considered the number of unoccupied sides as negligible, and the adsorption terms of isoamylenes, dimers and *n*-hexane showed the best fit. The number of active sites or clusters involved in the reaction surface step were, only one for dimerization, and three for trimerization. The best kinetic equations showed low sum of square residuals, appropriate residual randomness, low correlation between parameters and thermodynamic consistency. Finally, the activation energy for dimerization and trimerization were 37 and 89 kJ/mol, respectively, the dimerization activation energy being in the range of previous authors.

References

[1] I. Coleto, R. Roldán, C. Jiménez-Sanchidrián, J.P. Gómez, F.J. Romero-Salguero, Valorization of α-olefins: double bond shift and skeletal isomerization of 1-pentene and 1-hexene on zirconia-based catalysts, Catal. Today 149 (2010) 275–280.
[2] T.N. Mashapa, A. de Klerk, Solid phosphoric acid catalysed conversion of oxygenate containing Fischer–Tropsch naphtha, Appl. Catal. A 332 (2007) 200–208.
[3] R. Schmidt, M.B. Welch, B.B. Randolph, Oligomerization of C_5 olefins in light catalytic naphtha, Energy Fuels 22 (2008) 1148–1155.
[4] I. Coleto, R. Roldán, C. Jiménez-Sanchidrián, J.P. Gómez, F.J. Romero-Salguero, Transformation of α-olefins over Pt–M (M = Re, Sn, Ge) supported chlorinated alumina, Fuel 86 (2007) 1000–1007.

[5] V.J. Cruz, J.F. Izquierdo, F. Cunill, J. Tejero, M. Iborra, C. Fité, Acid ion exchange resins catalysts for the liquid-phase dimerization/etherification of isoamylenes in methanol or ethanol presence, React. Funct. Polym. 65 (2005) 149–160.
[6] V.J. Cruz, R. Bringué, F. Cunill, J.F. Izquierdo, J. Tejero, M. Iborra, C. Fité, Conversion, selectivity and kinetics of the liquid-phase dimerization of isoamylenes in the presence of C_1 to C_5 alcohols catalysed by a macroporous ion-exchange resin, J. Catal. 238 (2) (2006) 330–341.
[7] V.J. Cruz, J.F. Izquierdo, F. Cunill, J. Tejero, M. Iborra, C. Fité, R. Bringué, Kinetic modelling of the liquid-phase dimerization of isoamylenes on Amberlyst 35, React. Funct. Polym. 67 (2007) 210–224.
[8] M. Casagrande, L. Storano, M. Lenarda, S. Rossini, Solid acid catalysts from clays: oligomerization of 1-pentene on Al-pillared smectites, Catal. Commun. 6 (2005) 568–572.
[9] K. Föttinger, G. Kinger, H. Vinek, 1-pentene isomerisation over FER and BEA, Appl. Catal. A 249 (2003) 205–212.
[10] R. Catani, M. Mandreoli, S. Rossini, A. Vaccari, Mesoporous catalysts for the synthesis of clean diesel fuels by oligomerisation of olefins, Catal. Today 75 (2002) 125–131.
[11] M. Marchionna, M.D. Girolamo, R. Patrini, Light olefins dimerization to high quality gasoline components, Catal. Today 65 (2001) 397–403.
[12] M. Höchtl, A. Jentys, H. Vinek, Isomerization of 1-pentene over SAPO, CoAPO (AEL, AFI) molecular sieves and HZSM-5, Appl. Catal. A 207 (2001) 397–405.
[13] R.J. Quann, L.A. Green, S.A. Tabak, F.J. Krambeck, Chemistry of olefin oligomerization over ZSM-5 Catalyst, Ind. Eng. Chem. Res. 27 (1988) 565–570.
[14] J.C. Gee, S.T. Williams, Dimerization of linear olefins on Amberlyst 15: effects of chain length and double-bond position, J. Catal. 303 (2013) 1–8.
[15] A. de Klerk, Oligomerization of 1-hexene and 1-octene over solid acid catalysts, Ind. Eng. Chem. Res. 44 (2005) 3887–3893.
[16] M. Granollers, J.F. Izquierdo, J. Tejero, M. Iborra, C. Fité, R. Bringué, F. Cunill, Isoamylenes trimerization in liquid-phase over ion exchange resins and zeolites, Ind. Eng. Chem. Res. 49 (2010) 3561–3570.
[17] W.O. Haag, Oligomerization of isobutylene on cation exchange resins, Chem. Eng. Process. Symposium Series 73 (63) (1967) 140–146.
[18] K. Hauge, E. Bergene, D. Chen, G.R. Edriksen, A. Holmen, Oligomerization of isobutene over solid acid catalysts, Catal. Today 100 (2005) 463–466.
[19] A. Rehfinger, U. Hoffmann, Formation of di-isobutene, main by-product of methyl tertiary butyl ether synthesis catalyzed by ion exchange resin, Chem. Eng. Technol. 13 (1990) 150–156.
[20] M.L. Honkela, A.O.I. Krause, Kinetic modeling of the dimerization of isobutene, Ind. Eng. Chem. Res. 43 (13) (2004) 3251–3260.
[21] J.F. Izquierdo, M. Vila, J. Tejero, F. Cunill, M. Iborra, Kinetic study of isobutene dimerization catalyzed by a macroporous sulphonic acid resin, Appl. Catal. A 106 (1993) 155–165.
[22] N.F. Shah, M.M. Sharma, Dimerization of isoamylene: ion exchange resin and acid-treated clay as catalyst, Reactive Polym. 19 (1993) 181–190.
[23] M. Granollers, J.F. Izquierdo, F. Cunill, Effect of macroreticular acidic ion-exchange resins on 2-methyl-1-butene and 2-methyl-2-butene mixture oligomerization, Appl. Catal. A 435–436 (2012) 163–171.
[24] J.W. Yoon, J.S. Chang, H.D. Lee, T.J. Kim, S.H. Jhung, Trimerization of isobutene over cation exchange resins. Effect of physical properties of the resins and reaction steps, J. Mol. Catal. A: Chem. 260 (2006) 181–186.
[25] J. Gmehling, J. Li, M. Schiller, A modified UNIFAC model. 2. Present parameter matrix and results for different thermodynamics properties, Ind. Eng. Chem. Res. 32 (1993) 178–193.
[26] D.W. Marquardt, An algorithm for least-squares estimation of nonlinear parameters, J. Soc. Ind. Appl. Math. 11 (1963) 431–441.